ACADEMIA ROMÂNĂ
*Revue Roumaine de Chimie*
http://web.icf.ro/rrch/

*Rev. Roum. Chim.*
**2010**, *55*(1), 11-15

# INFLUENCE OF SODIUM IONS ($Na^+$) DOPANT ON THE EFFICIENCY OF THE TUNGSTEN TRIOXIDE PHOTOELECTRODE

Alexandru ENEŞCA,* Luminița ANDRONIC and Anca DUȚĂ

Transilvania University of Brasov, Faculty of Material Science and Engineering, Chemistry Department, Eroilor 29, 300056, Braşov, Roumania

*Received September 4, 2008*

The paper presents the influence of the sodium dopant ions ($Na^+$) on the properties of $WO_3$ film, used as photoelectrode for water photolysis. The photoluminescence and photocurrent stability were recorded in a photoelectrochemical system having doped and, respectively, undoped $WO_3$ films, deposited by spray pyrolysis on fluorine–doped tin oxide as photoanode and Pt as cathode, in electrolyte HCl (pH = 5). The crystalline structure, topography and electrical properties were investigated. The experiments confirm that the doping process doubles the photoelectrode efficiency.

## INTRODUCTION

There is a considerable interest in the research and development of materials and devices that can be used due to special opto-electronic properties. Several potential technologies are available for photocatalysis, including those based on the electrochromism, thermochromism and photochromism phenomena.[1] Since the first report on the photochromic properties of α-$WO_3$ by Deb,[2] in 1973, the preparation, microstructure and photochromic properties of WO3 have been studied because of the promising application in information display devices of high memory,[3-5] and in photocatalysis processes.[6-10] Photocatalysis can often be more accurately replaced by the term photosensitization, process in which light and a catalyst bring about or accelerate a chemical reaction.[11,12]

This paper presents results proving that the photoconversion efficiency of tungsten trioxide can be increased by inserting doping ions into the host lattice. The main effect of the doping process can be observed in the conductivity and photocurrent conversion efficiency. One of the major issues is the optimization of the dopant quantity that can improve the optoelectronic properties, without affecting the crystalline structure and the morphology of the native layer.[13]

## EXPERIMENTAL

### 1. Sample preparation

The FTO (fluorine doped tin oxide, $SnO_2$, coated glass – Libbey Owens Ford TEC 20/2.5 nm) was used as a substrate for $WO_3$ deposition. Samples of 2 x 2 $cm^2$ FTO (fluorine doped tin oxide) were cleaned by successive immersion in ethanol and acetone, using an ultrasonic bath, and dried with $N_2$ gas.

The precursor was prepared in three steps: (1) 0.05 M $(NH_4)_2WO_4$ was obtained by mixing $WO_3$ powder (99.8%, Alfa Aesar) with ammonium solution ( 25%, J.T. Baker) at the average temperature of 60˚C under continuous stirring using a reflux device, (2) 1 mL of acetilacetonate ($C_5H_8O_2$, 99.9%, Alfa Aesar) was added in the precursor solution as a complexion agent and (3) sodium chloride (NaCl, 99.9%, Alfa Aesar) was added as source of doping ions according to the doping ratio.

Four samples were prepared by SPD (spray pyrolysis deposition): one undoped sample (A1) and three doped samples at different atomic ratio (0.75 wt% - A2, 1.5 wt% - A3 and 3 wt% - A4). The deposition temperature was 350ºC as previously optimized,[14] and $N_2$ was used as inert carrier gas, at 1.5 bars. Samples were annealed in air, at 500°C, for 10 hours.[15]

### 2. Sample analysis

The X-Ray Diffraction (XRD) analysis was performed in grazing incidence method using a Bruker D8 Advance Diffractometer. The topography of the thin nanostructured films is studied using Atomic Force Microscopy (AFM, NT-MDT model BL222RNTE). The images were taken in contact mode with Si-tips (CSG10, force constant 0.15 N/m, tip radius10 nm).

The current-voltage, photoluminescence and photocurrent measurements are performed using a DC Source Meter

* Corresponding author: aenesca@unitbv.ro

(Keithley, model 2400), electronic diafragm (Uniblitz, model T132), tungsten/halogen lamp 250W (ThermoOriel, model 6334) and a monochromator (Acton Research Corporation, model 150 SpectraPro). The photoluminescence and photocurrent measurements use a cell with three electrodes: working electrode: doped or undoped $WO_3$ films immersed in electrolyte solution (HCl, pH = 5), counter electrode: platinum wire, and reference electrode: Ag/AgCl.

## RESULTS AND DISCUSSION

The advanced control of electrical and opto-electronic properties requires highly crystalline structures in the layers. The XRD (Fig.1) analysis shows the formation of monoclinic $WO_3$ in each sample and no other tungsten oxide states or sodium oxides were identified. The XRD pattern is similar for all samples regardless the dopant concentration proving that the thin films deposition conditions allowed the growth of doped tungsten oxide without other mixed compounds formation. Dopant ions will influence the crystallization degree of the host materials when the percentage of dopant is above 15% or when the dopant ions parameters (e.g. ionic radius $r_{Na+}$ = 1.02 Å, lattice structure) are very different compared with the tungsten ions ($r_{W6+}$ = 0.62 Å). Comparing with the undoped sample, the doped samples contain an extra peak attributed to the plane (022) and a lower intensity peak corresponding to the plane (400). Considering the network parameter values obtained form the diffraction analysis the cell volume increase with increasing the doping concentration (see table 1).

*Table 1*

Network parameters for doped and undoped films

| Samples | a (Å) | b (Å) | c (Å) | Network stress (ε) |
|---|---|---|---|---|
| A1 | 7.384 | 7.512 | 3.824 | 0.0038 |
| A2 | 7.274 | 7.501 | 7.543 | 0.0070 |
| A3 | 7.297 | 7.539 | 7.688 | 0.0090 |
| A4 | 7.297 | 7.539 | 7.688 | 0.0090 |

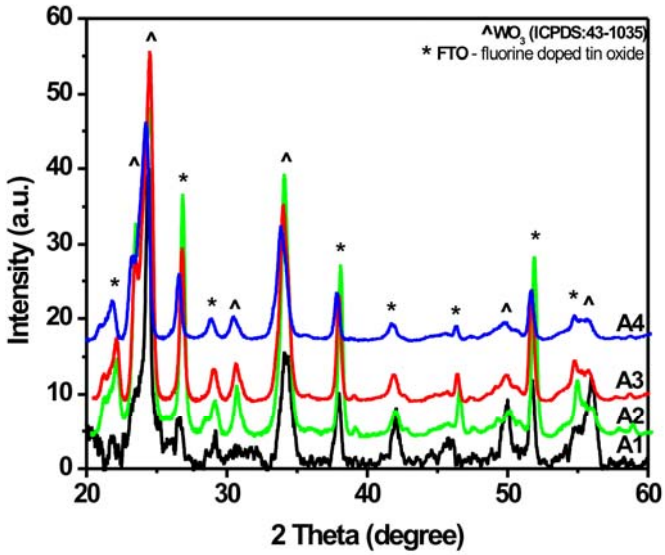


Fig. 1 – XRD spectrum of doped and undoped films.

The most likely process describing the defects formation involve only two types of defects that requires the lowest energy formation (in terms of charge and mobility) represented by oxygen vacancies and tungsten ions substitution with sodium ions. Oxygen vacancies are one of the most common defects; parts of them are passivated during the annealing process, decreasing the ionic conduction but increasing the electronic conduction.

The atomic force microscopy analysis (Fig. 2) shows a porous morphology (visible in 2D imagines) with homogeneity and uniformity on the films surface, characteristic for equal nucleation and growth rates during deposition. The surface is free of cracks or holes as results of the optimal

deposition and annealing parameters. The doping process does not alter the grains shape and size, while the roughness decrease for the doped samples (≈ 150nm for sample A2, A3 and A4) compared with the undoped sample (≈ 200nm for sample A1).

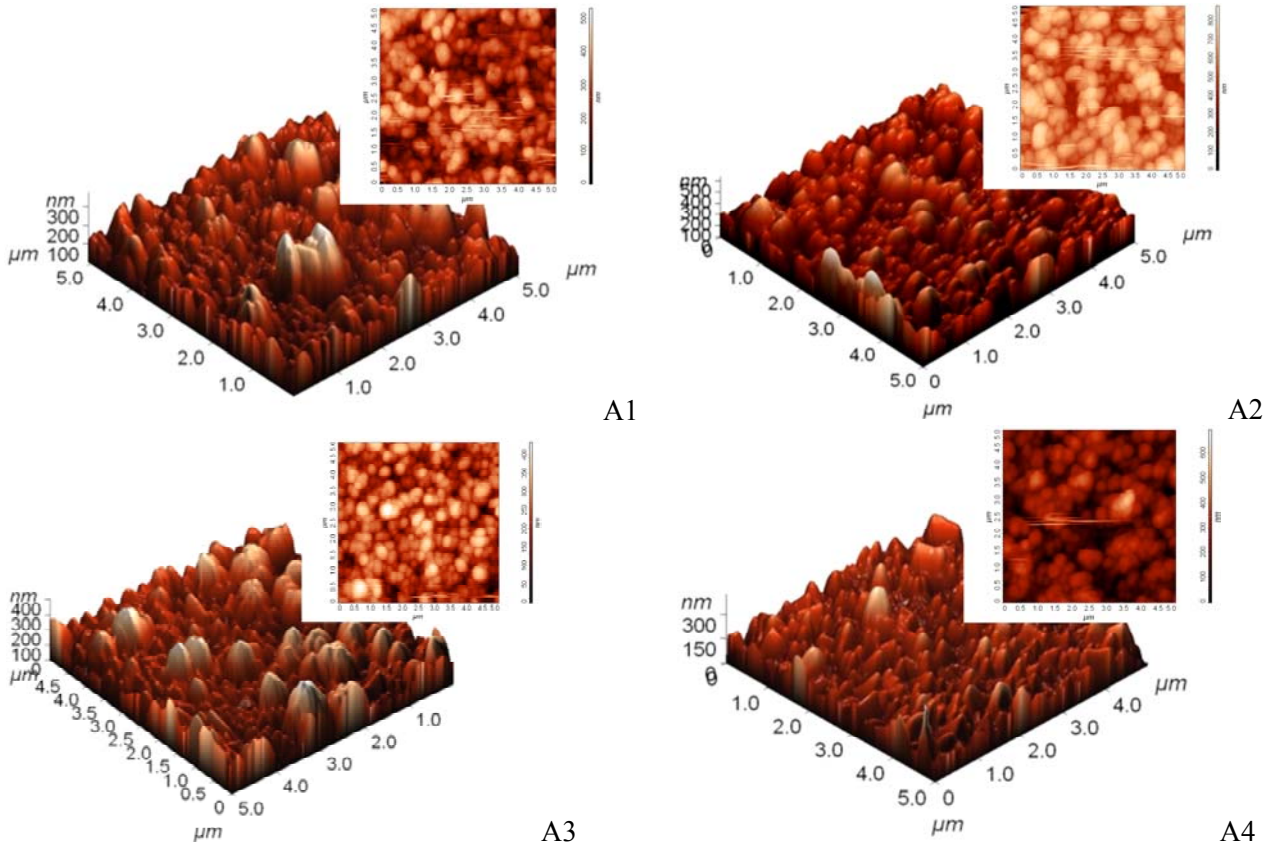


Fig. 2 – AFM 2D and 3D topographies of the samples.

In the photoelectrodes materials the morphology plays an important role regarding the oxide-electrolyte interface and has a direct influence on the system efficiency. The uniform grain distribution positively influences the chemical reactivity on each point of the surface.

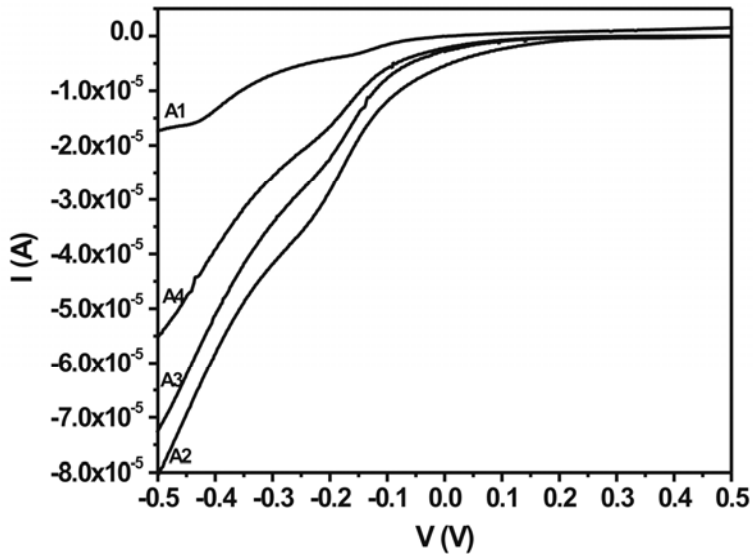


Fig. 3 – Conductivity analysis of doped and undoped samples.

The electrical properties where measured using current-voltage curves (Fig. 3) considering the changed induced by sodium ions (p type dopant, in this particular case) that will increase the influence of the electronic conductivity, compared with the ionic conductivity.

In doped samples the conductivity increase (sample A2) as the defect concentration decreases, consequence of the changes in Fermi energy level due to the electronic compensation processes. As a result of high dopant concentration (sample A4), the oxygen vacancy will increase the lattice deformation and, as consequence, the electrical resistance become higher.

The photoluminescence (Fig. 4) and photocurrent measurement indicate that the $WO_3$ doped with sodium ions have the required photoanodes properties necessaries to function into a photo-electrochemical cells (PECC). The acid electrolyte was chosen considering the $WO_3$ chemical stability in this environment.[15] Regardless the samples (doped or undoped) if the value of the applied voltage is 0 V, the films have no photoresponse under irradiation. If the external voltage is risen up to 0.5 V, the light sensitivity properties are activated and the photocurrent response is detected. The total absorption wavelength is recorded between 300 - 450nm and the maximum photocurrent response is present at 380 nm. The sample A2 present higher photocurrent intensity compared with samples A1, A3 and A4 due to the proper balance between the dopant concentration and electronic compensation.

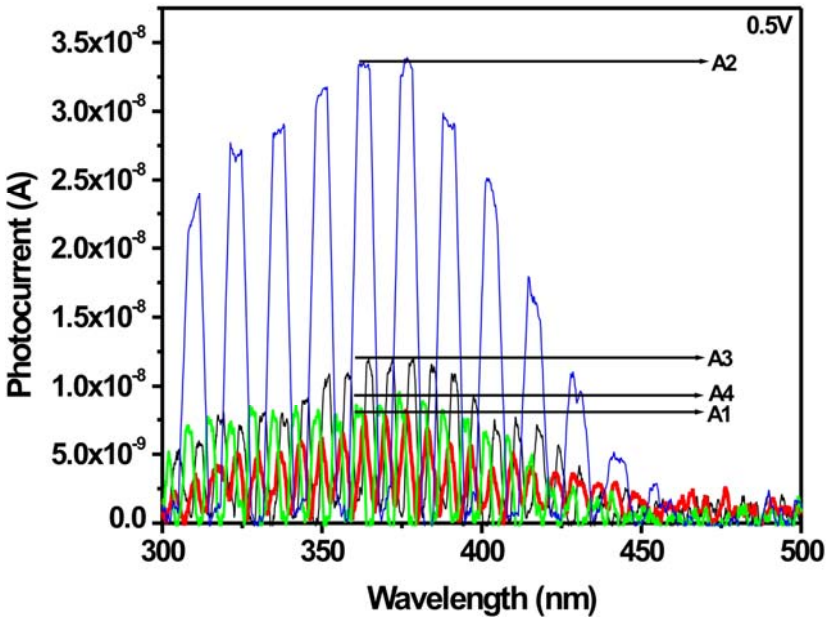


Fig. 4 – Photoluminescence spectrum of the samples.

This results are reflected in the photocurrent measurement (Fig. 5) made at 375 nm under an external bias of 0.5 V. The samples shows a fast response (1-2s) and photocurrent stability, considering that the measurements are developed in an electrolyte, favoring interface changes.

The efficiency of water splitting process is influenced by the dopant concentration (Fig. 5). The samples doped with 3% sodium ions have a lower efficiency compared with the undoped sample. The $WO_3$ films doped with 0.75% sodium ions have a higher efficiency comparing with sample A3 and A4 and almost double comparing with the undoped sample. The doping process involves two major effects regarding the photocurrent response: (1) changes at film-electrolyte interface induced by the high oxygen vacancy concentration, and (2) changes in the bulk conductivity. The optimization of dopant concentration in $WO_3$ lattice will assure the balance between these two effects.

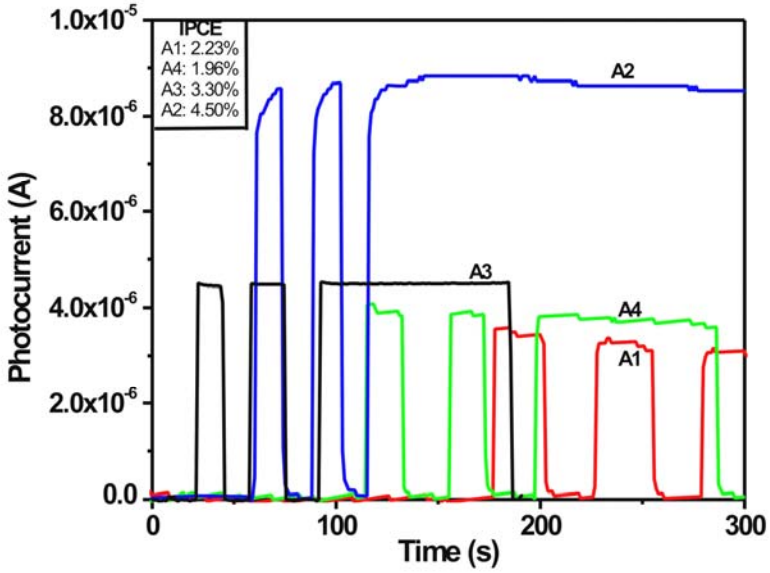


Fig. 5 – Photocurrent evolution in time.

## CONCLUSION

Thin $WO_3$ films doped with sodium ions in different concentrations (A2 – 0.75%, A3 - 1.5% and A4 - 3 wt%), were prepared using spray pyrolysis as deposition technique and annealed as post-deposition treatment. Even if the sodium ionic radius is different compared with tungsten ionic radius the diffraction analysis and opto-electrical measurements prove the proper insertion of doping ions in the host lattice.

The samples have porous morphology, with good uniformity and homogeneity. The electrical conduction decreases as the dopant concentration increase due to the electronic compensation. The photocurrent is present between 300 – 450nm with a maximum at 380nm. The sample with the lowest sodium content presents a higher photoconversion efficiency comparing with the other doped and undoped samples due to the balance between the interface process and bulk properties.

*Acknowledgements:* This work was supported by the Roumanian National Council for Research in High Education according with the CNCSIS ID-753/2008 grant.

## REFERENCES

1. C.G. Granquivist, "Handbook of Inorganic Electrochromic Materials", Elsevier, Amsterdam, 1995, p. 180 - 201.
2. S.K. Deb, *Philos. Mag.,* **1973,** *22,* 801-804.
3. N. Xu, M. Sun, Y.W. Cao, J.N. Yao and E.G. Wang, *Appl. Surf. Sci.,* **2000,** *157,* 81-84.
4. T. Oi, K. Miyauchi and K. Uehara, *J. Appl. Phys.,* **1982,** *53,* 1823-1826.
5. C.O. Avellaneda and L.O.S. Bulhoes, *Solid State Ionics,* **2003,** *165,* 117-200.
6. A. Fujishima and K. Honda, *Acc. Chem. Res.,* **1995,** *28,* 3-8.
7. M. Kamei and T. Mitsuhushi, *Surf. Sci.,* **2000,** *L609,* 463-468.
8. A. Rampaul, I.P. Parkin, S.A. O'Neill, J. DeSouza, A. Mills and N. Elliott, *Polyhedron,* **2003,** *22,* 35-38.
9. M. Valigi, D. Gazzoli, I. Pettiti, G. Mattei, S. Colonna, S. De Rossi and G. Ferraris, *Appl. Cat. A: General,* **2002,** *231,* 159 - 164.
10. I. Porqueras and E. Bertran, *Thin Solid Films,* **2000,** *129,* 377 -380.
11. S.Zh. Karazhanov, Y. Zhang, L.-W. Wang, A. Mascarenhas and S. Deb, *Phys. Rev. B: Condens. Matter Mater. Phys.,* **2003,** *68,* 233204-233207.
12. P. Lindan, E. Duplock, C. Zhang, M. Thomas, R. Chatten and A. Chadwick, *Dalton Trans.,* **2004,** *3,* 65-70.
13. E. Pehlivan, F.Z. Tepehan and G.G. Tepehan, *Solid State Ionics,* **2003,** *165,* 105-108.
14. A. Enesca, C. Enache, A. Duta and J. Schoonman, *J. Eur. Ceram. Soc.,* **2006,** *26,* 571-574.
15. A. Enesca, A. Duta and J. Schoonman, *Thin Solid Films,* **2007,** *515,* 6371-6374.